Room-Temperature Ferromagnetism in Mn-Doped Semiconducting CdGeP$_2$

Priya Mahadevan and Alex Zunger

National Renewable Energy Laboratory, Golden, Colorado 80401

The chalcopyrite CdGeP$_2$ doped with Mn have been recently found to exhibit room-temperature ferromagnetism. Isovalent substitution of the Cd site is expected, however, to create *antiferromagnetism*, in analogy with the well-known CdTe:Mn (d^5) case. However, chalcopyrite semiconductors exhibit low-energy *intrinsic* defects. We show theoretically how ferromagnetism results from the interaction of Mn with hole-producing intrinsic defects.

Spintronics [1]—the use of spin rather than charge in electronics—calls for room-temperature ferromagnetism (FM) in a semiconductor. Despite several attempts to dope semiconductors with transition metal atoms [2], most of them did not show magnetic ordering. The dopant of choice here [3] is Mn^0 ($d^5 s^2$), being formally Mn^{2+} (d^5) when substituting a divalent cation, and Mn^{3+} (d^4) when replacing a trivalent cation. Mn on the divalent cation site of II-VI semiconductors is attractive because of the significant solubility of the isovalent Mn^{2+}, but this produces antiferromagnetism (AFM) [4]. The reason is that in a ferromagnetic arrangement all 3d spin-up orbitals are occupied so there is no empty orbital on a neighboring Mn atom for the electron from one Mn atom to hop onto. Therefore an antiferromagnetic arrangement of spins at neighboring Mn sites is favored. The III-V compounds doped with Mn would have been suitable candidates for FM as these systems are known [5] to have holes ($d^4 \rightarrow d^5$ + hole) when Mn^{3+} substitutes the trivalent cation site. However, the ferromagnetic transition temperature (T_c) in these compounds is limited by the fact that Mn^{3+} has low solubility [3], and above a critical concentration ($\sim$8% in GaAs) tends to cluster and phase separate. This was not a limitation while doping the II-VI semiconductors. Recently, Medvedkin *et al.* [6] came up with the novel idea of obtaining both high solubility and high T_c in a semiconductor: replacing Cd sites in the chalcopyrite CdGeP$_2$ with Mn atoms. Although CdGeP$_2$ is isovalent to the III-V compounds [7] (the average valence of Cd and Ge is a group III element), a large amount ($\sim$50% at the surface) of Mn could be doped into this system, resulting in FM in a semiconductor at 320 K [6]. However, the existence of FM in CdGeP$_2$:Mn is surprising since, as explained above, replacement of a divalent site by Mn^{2+} (d^5) is known [4] to give rise to an antiferromagnetic interaction between the Mn atoms. Indeed, recent electronic structure calculations [8] found that Mn-doped CdGeP$_2$ was antiferromagnetic, just as Mn-doped CdTe [9]. We show here that Mn doping in CdGeP$_2$ can produce stable FM. This hitherto unexplored unusual form of FM results from the interaction of a magnetic ion such as Mn with holes produced by *intrinsic defects*. The central point is that chalcopyrite semi-

conductors are known [10] to be stabilized by certain intrinsic defects such as cation (Cd,Ge) vacancies, vacancy-antisite pairs, and the presence of hole-producing defects which could result in FM being favored even when Mn dopes the Cd site. The theoretical challenge is to identify the hole-producing defects that form stable complexes with substitution. In this work we have calculated the formation energies of various kinds of defects and predicted the conditions favoring the substitution of Cd sites and Ge sites by Mn. From this we infer that FM is induced by holes generated in structures resulting from the simultaneous substitution of both Cd and Ge sites or the substitution of only the Ge sites with Mn. This offers a novel design principle for obtaining both high Mn solubility and high-T_c FM due to defect-induced hole production in semiconducting systems.

We first calculated the formation energies of intrinsic point defects such as a vacancy at a Cd site (V$_{Cd}$), a vacancy at a Ge site (V$_{Ge}$), and a Ge antisite on Cd (Ge$_{Cd}$), finding the energetically stablest defects. Then we calculate formation energies for Mn substituting a Cd site (Mn$_{Cd}$) and a Ge site (Mn$_{Ge}$). Finally, we deduce which of the many possible complexes would have simultaneously low formation energy (hence, high concentration) and create hole states (therefore coupling the Mn atoms ferromagnetically).

We performed plane-wave pseudopotential [11–13] calculations with isolated defects/Mn atoms introduced into 64 atom supercells of CdGeP$_2$. The lattice parameters of these supercells were fixed at the theoretically calculated values for CdGeP$_2$: $a = 5.81$ Å and $c = 10.96$ Å; while the atomic positions were relaxed. The formation energy for a defect comprising atoms α in the charge state q was computed using the expression [10]

$$\Delta H_f(\alpha, q) = E(\alpha) - E(0) + \sum_\alpha n_\alpha \mu_\alpha^a + q(E_{\text{VBM}} + \epsilon_f), \qquad (1)$$

where $E(\alpha)$ and $E(0)$ are the total energies of the supercell with and without defect α. n_α is the number of each defect atom; $n_\alpha = -1$ if an atom is added, while $n_\alpha = 1$ if an

atom is removed. μ_α^a is the absolute value of the chemical potential of atom α. Since the formation energies are conventionally defined with respect to the elemental solid(s), we express μ_α^a as the sum of a component due to the element in its most commonly occurring structure μ_α^s, and an excess chemical potential μ_α, i.e., $\mu_\alpha^a = \mu_\alpha^s + \mu_\alpha$. Here μ_α^s for P, Ge, Mn, and Cd are the total energies evaluated for the fully optimized elemental solids in the observed crystal structures [14]. If $\Delta H_f(CdGeP_2)$ is the formation energy of $CdGeP_2$, then μ_{Cd} and μ_{Ge} are determined by

$$\mu_{Cd} + \mu_{Ge} + 2\mu_P \leq \Delta H_f(CdGeP_2). \qquad (2)$$

Furthermore, $\mu_{Cd} \leq 0$; $\mu_{Ge} \leq 0$, because otherwise the elemental solids will precipitate. The presence of other intervening binary phases, however, further restricts the values of μ_{Cd} and μ_{Ge}: One must solve Eq. (2) along with the constraints placed by the formation energies $\Delta H_f(Cd_3P_2)$ and $\Delta H_f(GeP)$ of Cd_3P_2 and GeP:

$$3\mu_{Cd} + 2\mu_P \leq \Delta H_f(Cd_3P_2), \qquad (3)$$

$$\mu_{Ge} + \mu_P \leq \Delta H_f(GeP), \qquad (4)$$

to find the allowed range for μ_{Cd} and μ_{Ge} in $CdGeP_2$. The electrons ionized upon forming a positively charged defect join the Fermi sea so the formation energy increases by $q\epsilon_f$, where ϵ_f is the fermi energy which varies from 0 eV at the valence band maximum (VBM) of the host material to the band gap of the host. Equations (2)–(4) were solved using the experimental values [15,16] of the formation energies for the binary phases Cd_3P_2 (-1.2 eV) and GeP (-0.3 eV), while a value of -1.5 eV, in the same range as other chalcopyrites [17], was used for $CdGeP_2$.

The allowed range of chemical potentials μ_{Cd} and μ_{Ge} for $CdGeP_2$ and the binaries Cd_3P_2 and GeP are given in Fig. 1. There are three distinct chemical potential domains where $CdGeP_2$ can exist: point A: Cd rich, Ge poor;
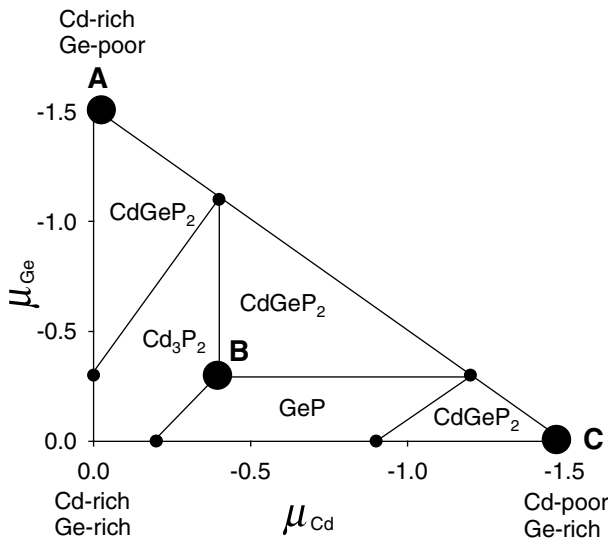
point B: Cd rich, Ge-rich; and point C: Cd poor, Ge rich. Figure 2 shows the formation energies of the intrinsic point defects Ge_{Cd}, V_{Cd}, and V_{Ge} as well as substitutional defects Mn_{Ge} and Mn_{Cd} at the chemical potentials A, B, and C of Fig. 1 as a function of the Fermi energy. The vertical dashed line denotes the generalized gradient approximation (GGA) gap which is underestimated with respect to the experimental 1.72 eV gap. Transition points between charge states are indicated by solid circles. The defects can form acceptor states generating holes in the system [e.g., $(-/0)$ or $(2-/-)$] or donor states that generate electrons [e.g., $(0/+)$]. We see that (i) when $CdGeP_2$ is grown at point C (Cd poor and Ge rich), and to a lesser extent at point B (Cd rich and Ge rich), the favored substitution of Mn is on the Cd site. This substitution leads to a neutral charge state (no holes), thus to AFM. (ii) However, for n-type conditions (E_F near the conduction band maximum) at point B, and at all E_F values at point A (Cd rich; Ge poor), the stablest site for Mn substitution is the Ge site. This substitution forms both single and double hole-producing acceptors, which can promote FM. However, under n-type conditions at point B, the charge state $q = -2$ is favored, which has no holes and therefore promotes AFM. Analysis of the wave functions for different eigenvalues revealed that the Mn $3d$ levels are located 2–3 eV *below* the VBM and so one spin channel is fully filled (five electrons). While formally Mn^{4+} would have a d^3 configuration, the existence of a fully occupied d^5 implies that two electrons are captured from the states near ϵ_f. The levels which are emptied correspond to the acceptor transitions taking place at 0.5 and 0.57 eV above E_{VBM}. (iii) Cadmium vacancies with the charge state $q = -2$ are easily formed (in n-type conditions) at points A and C. (iv) Ge vacancy is stable for n-type conditions of point A, though the charge state which has the lowest energy

FIG. 1. The range of Cd and Ge chemical potentials where $CdGeP_2$, GeP, and Cd_3P_2 are stable.
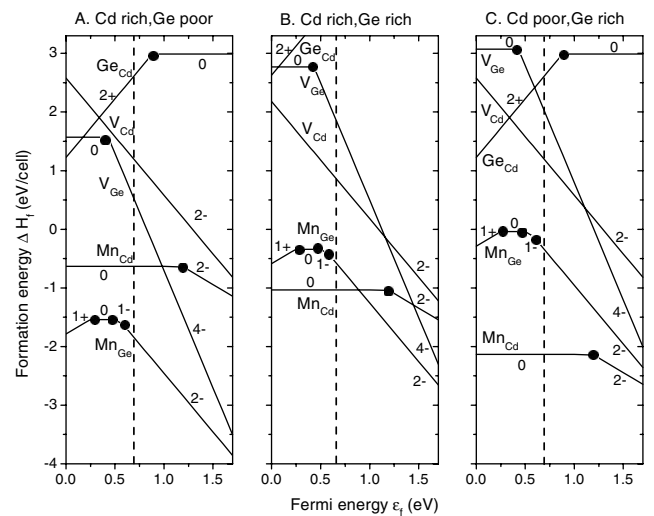
FIG. 2. The calculated formation energies as a function of fermi energy for different charge states of isolated defects in a 64 atom cell of $CdGeP_2$ for chemical potentials: (A), (B), and (C). The vertical dashed line (solid circle) denotes the calculated GGA band gap (transition energy between charge states).

in these conditions has no holes and so cannot promote antiferromagnetism. (v)Ge-on-Cd antisite has high formation energy, and would therefore not have appreciable concentration.

Having identified the hole-producing centers that can yield FM, we next examine the predicted solubilities of isolated Mn. Our calculated formation energies for $CdGeP_2$:Mn and similar calculations for GaAs:Mn show consistently lower values (for the appropriate chemical potentials) in the former case, predicting higher Mn solubility: The lowest formation energy of substituting a Ga atom with Mn in GaAs is 1.0 eV (under Mn-rich, Ga-poor conditions). In contrast, even in the worst-case scenarios, we find a value of $\Delta H_f \sim -0.6$ eV for Mn_{Cd} in $CdGeP_2$ under Cd-rich, Ge-poor conditions. For Mn_{Ge}, we find $\Delta H_f \sim 0$ eV under Cd-poor, Ge-rich conditions.

Having established low substitution energies for Mn in $CdGeP_2$, we next see if Mn tends to cluster or not. We calculated the pairing energy, δ, of a pair relative to infinitely separated Mn atoms in the host, given by $\delta = [E(2Mn) - E(0Mn)] - 2[E(1Mn) - E(0Mn)]$, where $E(n\,Mn)$ is the total energy of the supercell with n Mn atoms. A negative pairing energy would imply that the two Mn atoms would prefer to pair rather than stay far apart. The pairing energy for nearest neighbor Mn_{Cd} and Mn_{Ge} pairs were found to be $+577$ meV and $+513$ meV, respectively, for the unit cell considered, implying no clustering. On the other hand, Mn substitution of GaAs had a negative pairing energy, equal to -250 meV for Mn occupying nearest neighbor Ga sites. The corresponding energy for clusters of three or four Mn occupying the vertices of a tetrahedron surrounding a single As in GaAs was even more negative, indicating that the Mn atoms showed a tendency of forming clusters when introduced into GaAs. The Mn atoms doped into $CdGeP_2$ did not exhibit this tendency.

Having established that the (i) isolated defects Mn_{Cd}, Mn_{Ge}, and V_{Cd} have the lowest formation energy under certain specified experimental conditions, and (ii) for some charge states the latter two are hole producing (and therefore potentially FM promoting), and that (iii) Mn_{Ge} pairs repel each other rather than cluster, we now examine (iv) the various combinations of these point defects in search of stable, hole-producing *complexes*. Two Mn atoms were introduced along with various intrinsic defects at various positions of 16 as well as 32 atom supercells of $CdGeP_2$ corresponding to 50% and 25% Mn, respectively. The energies of the ferromagnetic and antiferromagnetic arrangements were computed for the fully optimized supercell. The formation energies of the defect complexes in the 32 atom unit cell are plotted in Fig. 3 as a function of μ_{Cd} [panel 3(a)] and μ_{Ge} [panel 3(b)] with the magnetic ground state (A = AFM and F = FM) indicated in parentheses for the defect complex with the lowest energy. The vertical arrows denote the values of chemical potential for which there is a crossover in the type of defect with the lowest energy. We see that (i) under Ge-rich conditions, where *isolated* Mn prefers the Cd site [Fig. 2(c)], a pair of Mn atoms also prefers the Cd site [Fig. 3(a)], leading to an AFM ground state. For 25% Mn, the antiferromagnetic state is lower in energy than the ferromagnetic state by 105, 19, 13, and 15 meV/Mn for Mn_{Cd}-Mn_{Cd} separations of first, second, third, and fourth neighbors, respectively, which changes from 124 to 23 meV/Mn for first and second neighbors at 50% doping. The energy difference for the second neighbor positions are in agreement with the difference of 21 and 35 meV obtained by earlier calculations [8] for 25% and 50% dopings. (ii) Adding a Cd vacancy to the Mn_{Cd}-Mn_{Cd} pair lowers the energy for the Cd-poor range of Fig. 3(a), but leaves the system antiferromagnetic. (iii) Under Cd-rich conditions, where *isolated* Mn prefers the Ge site [Fig. 2(a)], a pair of Mn atoms also prefers the Ge site [Fig. 3(b)], except at the very Ge-rich end. For 25% Mn, the FM state is lower in energy than the AFM state by 111, 67, and 82 meV/Mn for Mn_{Ge}-Mn_{Ge} separations of first, second, and third neighbors, respectively. For the 50% Mn case, the ferromagnetic state is still stable by 131 and 158 meV/Mn for first and second neighbors. The fact that the energy difference between the ferromagnetic and the antiferromagnetic states is quite large even when Mn atoms are at third neighbor separation implies that the magnetic interactions are long ranged in this case, unlike when Mn dopes the Cd site. (iv) The combination of Mn_{Cd}-Mn_{Ge} pairs is also ferromagnetic, being comparable in energy to when Mn replaces the Ge sites for certain chemical potentials of Fig. 3(b).

In pure $CdGeP_2$, the valence electron configuration is $a^2 t_p^6$, where p denotes the dominant character of the level. This reflects the fact that Ge contributes one electron to each of the four bonds with P, Cd contributes $\frac{1}{2}$ electron, and P contributes $\frac{5}{4}$ electrons; the GeP_4 tetrahedron transfers one electron to the CdP_4 tetrahedron, through the bridging P. The electronic structure of a transition metal substituting a cation site in a semiconductor can be described by the hybridization between the orbitals of the transition metal ion and the anion dangling bonds formed from the cation vacancy in the host semiconductor [2]. Figure 4 shows this for Mn_{Ge} in $CdGeP_2$. The up-spin $(+)$
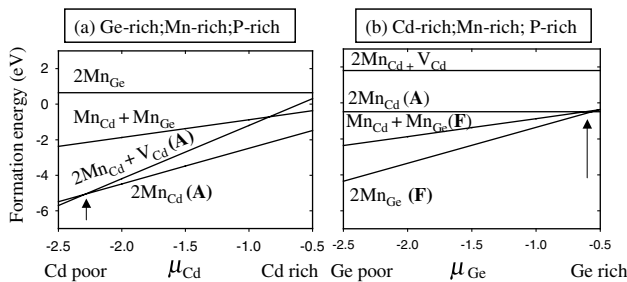
FIG. 3. The formation energies as a function of (a) Cd and (b) Ge chemical potentials calculated for complex defects in a 32 atom cell of $CdGeP_2$. The magnetic ground state (A = AFM, F = FM) for the lowest energy state is indicated. The vertical arrows denote the value of chemical potential for which there is a crossover in the lowest energy defect type.
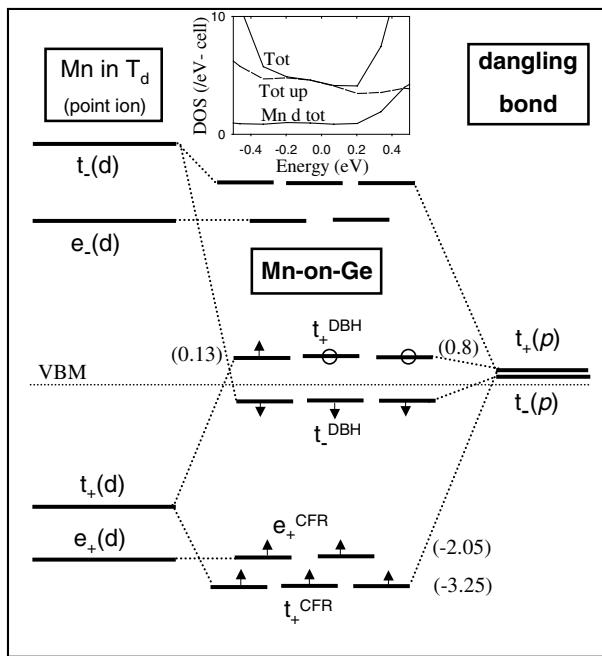
FIG. 4. The energy level diagram of Mn_{Ge} in $CdGeP_2$ (energy of the levels in brackets). The inset shows the contributions to the total DOS from the up spin as well as Mn $3d$ states calculated for 2 Mn_{Ge} in a 32 atom unit cell of $CdGeP_2$.

levels with t character on Mn (left) hybridize with the levels with the same symmetry on the Ge-vacancy dangling bond (right), thus forming a bonding "crystal field resonance" (CFR) t_+^{CFR} located deep in the valence band with dominant Mn character, and antibonding "dangling bond hybrid" (DBH) t_+^{DBH} with dominantly P p character. A similar hybridization of the down-spin ($-$) levels results in the down-spin counterparts of the CFR and DBH levels. The CFR level with e symmetry exists also. When Mn is substituted on the Ge site, four of its seven valence electrons replace those of Ge, leaving three electrons to occupy t_+^{CFR} and e_+^{CFR}. However, since t_+^{DBH} is higher in energy than e_+^{CFR}, two electrons move into e_+^{CFR} and so two holes (empty circles in Fig. 4) are generated in the DBH levels. The intra-atomic exchange splitting on the Mn atoms is large, ~ 0.6–0.7 eV [18], and a large negative (0.8–1.0 eV) exchange splitting is induced on the DBH levels (Fig. 4). For an isolated Mn impurity, as both spin channels are partially occupied, the energy gain as a result of hybridization has contributions from both spin channels. While this exchange splitting and therefore the energy gain is enhanced for a ferromagnetic arrangement of Mn spins, similar hybridization arguments will show that they are reduced in an antiferromagnetic arrangement of Mn spins. Consequently, ferromagnetism is favored. The mechanism is similar to that proposed earlier to explain the high T_c observed in another ferromagnet where the magnetic Fe atoms are separated by nonmagnetic Mo atoms [19]. In the inset of Fig. 4, we show the contributions to the total density of states (DOS) from the up-spin states as well as

the Mn d states in a small energy window near the Fermi energy. The states are found to be strongly spin polarized, with just 25% Mn d character from the two Mn atoms present in the 32 atom supercell considered here. As a result of the large exchange splitting induced on the DBH states, the down-spin DBH bands move into the valence band of the host. The strongly polarized as well as delocalized down-spin DBH band, we believe, is responsible for the long-ranged magnetic interactions, and, consequently, the room temperature FM found in Mn-doped $CdGeP_2$.

[1] T. Dietl et al., Science **287**, 1019 (2000); T. Dietl, J. Appl. Phys. **89**, 7437 (2001).
[2] A. Zunger, in Solid State Physics (Academic, New York, 1986), Vol. 39, p. 275.
[3] H. Munekata et al., Phys. Rev. Lett. **63**, 1849 (1989).
[4] J. K. Furdyna and J. Kossut, Semiconductors and Semimetals (Academic, San Diego, 1988), Vol. 25.
[5] J. Schneider et al., Phys. Rev. Lett. **59**, 240 (1987).
[6] G. A. Medvedkin et al., Jpn. J. Appl. Phys., Part 2 **39**, L949 (2000).
[7] J. E. Jaffe and A. Zunger, Phys. Rev. B **30**, 741 (1984).
[8] Yu-Jun Zhao, W. T. Geng, A. J. Freeman, and T. Oguchi, Phys. Rev. B **64**, 035207 (2001).
[9] S. H. Wei and A. Zunger, Phys. Rev. B **35**, 2340 (1987).
[10] S. B. Zhang, S. H. Wei, and A. Zunger, Phys. Rev. Lett. **78**, 4059 (1997); S. B. Zhang, S. H. Wei, A. Zunger, and H. Katayama-Yoshida, Phys. Rev. B **57**, 9642 (1998).
[11] The pseudopotential plane-wave method [12] using GGA PW91 ultrasoft pseudopotentials as implemented in VASP [13] was used. Cutoff energies of 16.7 Ry (28.2 Ry) and 15.9 Ry (20.2 Ry) were used for the plane-wave (augmentation charge) for the calculations with and without Mn, respectively. A Monkhorst-Pack k-points grid of $4 \times 4 \times 2$, $2 \times 4 \times 2$, and $2 \times 2 \times 2$ was used for the calculations involving 16, 32, and 64 atoms.
[12] J. Ihm, A. Zunger, and M. L. Cohen, J. Phys. C **12**, 4409 (1979).
[13] G. Kresse and J. Furthmüller, Phys. Rev. B **54**, 11 169 (1996); G. Kresse and J. Furthmüller, Comput. Mater. Sci. **6**, 15 (1996).
[14] P. Villars and J. L. Calvert, Pearsons Handbook of Crystallographic Data for Intermetallic Phases (ASM International, Materials Park, 1991).
[15] NBS Tables of Chemical Thermodynamic Properties, edited by D. Wagman et al. (ACS and AIP for the National Bureau of Standards, Washington, DC, 1982), Vol. 11.
[16] The use of calculated formation energies (Cd_3P_2: -1.3 eV; GeP: $+0.33$ eV; $CdGeP_2$: -0.93 eV) does not change the conclusions of our work.
[17] L. I. Berger, Semiconductor Materials (CRC Press, New York, 1997), p. 230.
[18] P. Mahadevan, N. Shanthi, and D. D. Sarma, J. Phys. Condens. Matter **9**, 3129 (1997).
[19] D. D. Sarma et al., Phys. Rev. Lett. **85**, 2549 (2000).